USING LEAD ISOTOPES AND ELEMENTAL ABUNDANCES IN TILL FOR MINERAL EXPLORATION IN CORDILLERA

Alexei S. Rukhlov and Travis Ferbey

British Columbia Geological Survey, Ministry of Energy and Mines, 1810 Blanshard Street, Victoria, British Columbia, V8W 9N3

BRITISH COLUMBIA Ministry of Energy and Mines

For More Information:
(250) 952-0396
Alexei.Rukhlov@gov.bc.ca

Recommended citation:
Rukhlov, A.S., Ferbey, T., 2015. Using lead isotopes and elemental abundances in till for mineral exploration in Cordillera. British Columbia Ministry of Energy and Mines, British Columbia Geological Survey GeoFile 2015-01.
http://www.empr.gov.bc.ca/Mining/Geoscience/PublicationsCatalogue/GeoFiles/Pages/GF2015-1.aspx

ABSTRACT

Elemental abundances and Pb isotopic ratios for 2.5N HCl leachates from Chehalis valley basal till samples (<0.063 mm fraction) highlight down-ice glacial dispersal for volcanogenic massive sulphide (VMS) occurrences. In spite of the relatively young age of the VMS deposit and surrounding volcanic-arc rocks (middle Jurassic), the Pb isotopic ratios show 3-9% difference between the ore and the background crustal samples. This is 2-3 orders of magnitude above the analytical uncertainties of the state-of-the-art multi-collector inductively coupled plasma mass spectrometry (MC-ICP-MS) after Pb purification by ion-exchange separation. The simplified method, measuring Pb isotopic ratios directly in bulk 2.5N HCl leachate solution by high-resolution inductively coupled plasma mass spectrometry (HR-ICP-MS), also has acceptable analytical uncertainties (0.4-0.6%) for the $^{206}Pb/^{204}Pb$ and $^{207}Pb/^{206}Pb$, tracing down-ice dispersal, consistent with the MC-ICP-MS results. For the direct-leachate analyses using quadrupole ICP-MS, the analytical uncertainties of the uncorrected for mass bias Pb isotopic ratios (2-9 times those of the HR-ICP-MS and 200-300 times those of MC-ICP-MS) may be too large for the applications requiring <10% resolution. Although Pb, Zn, Cu, and Ba abundances are enriched in the Seneca VMS deposit (10-1000 times typical crustal values), they show inconsistent down-ice till anomalies. In contrast, Pb isotopic ratios for leachates from <0.063 mm fraction of the tills appear to be robust indicators of down-ice glacial dispersal for the VMS mineralization. The Pb abundances and isotopic compositions are consistent with the model that Chehalis valley tills are derived from the isotopically heterogeneous local bedrock sources and have variable proportions of lead from the VMS mineralization. The latter has low $^{206}Pb/^{204}Pb$, $^{207}Pb/^{204}Pb$, and $^{208}Pb/^{204}Pb$, and high $^{207}Pb/^{206}Pb$ and $^{208}Pb/^{206}Pb$ ratios that are similar to those of galena from the Seneca deposit (Godwin, 1988). The slope of the $^{207}Pb/^{204}Pb$ vs. $^{206}Pb/^{204}Pb$ near-linear array defined by Chehalis till and rock samples (n = 13, excluding diorite from Mt. Jasper pluton) corresponds to a secondary isochron age of 2131±180 Ma, with the lower intercept of the Stacey and Kramers (1975) growth curve at 2271 Ma. This is much older than the emplacement age of the Seneca VMS deposit and the surrounding volcanic-arc rocks but falls within the range of the Paleoproterozoic ages of the major crust-forming events worldwide. If the near-linear array had a geochronological significance, it would imply that both the Seneca VMS deposit and the surrounding volcanic rocks shared the same, closed-system Paleoproterozoic source, such as a sub-continental lithosphere.

INTRODUCTION

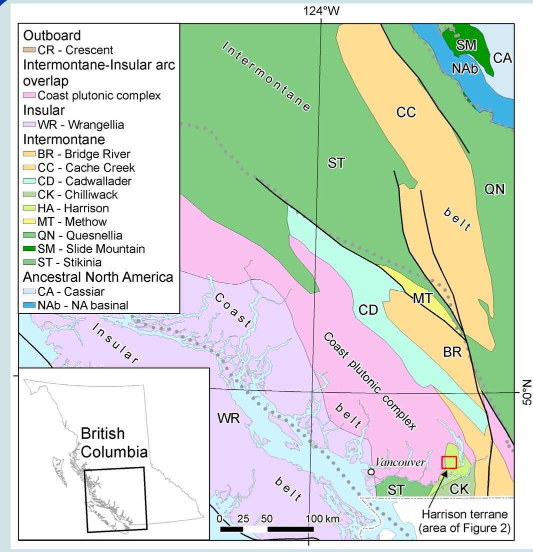

Figure 1. Terranes (after Colpron and Nelson, 2011) and location of Chehalis valley study area (red box) in southwestern British Columbia. Dotted lines show boundaries of the morphogeological belts after Gabrielse et al. (1991).

Basal till is a primary bedrock-derived sediment, with little or no reworking by water, transported and re-deposited at the base of a glacier by near-linear, and often valley-parallel, ice flow during one or more episodes of Quaternary glaciation (Levson, 2001). Lithological, mineralogical and geochemical anomalies within this sediment, resulting from the erosion and down-ice glacial transport of compositionally distinct bedrock, have been widely used as indicators of glacial dispersal for mineral exploration (e.g., Shilts, 1976, DiLabio, 1990). Previous studies have shown that Pb isotopic ratios from 2.5N HCl leachates from <0.063 mm fraction of basal till can be the effective indicators of glacial dispersal for Paleoproterozoic and early Paleozoic VMS deposits (Bell and Franklin, 1993; Bell and Murton, 1995; Simonetti et al., 1996). We have analyzed 26 till samples (<0.063 mm fraction) and 11 bedrock samples from Chehalis valley, southwestern British Columbia (Fig. 1), for Pb isotopic ratios and elemental abundances to test: (1) the effectiveness of Pb isotopes for tracing glacial dispersal from as young as the middle Jurassic VMS deposits, and (2) the suitability of different instrumentation for the Pb isotopic analysis of 2.5N HCl leachates from tills.

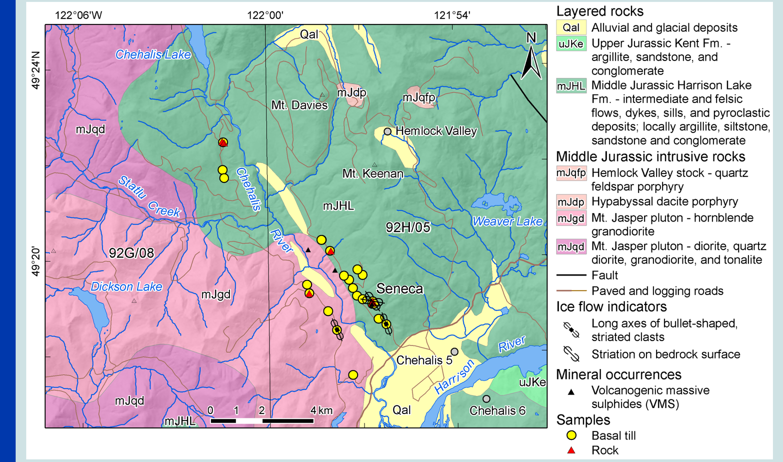

Figure 2. Geology, sample locations, ice-flow indicators and mineral occurrences, Chehalis valley study area, southwestern British Columbia. Geology after Monger (1970), Arthur et al. (1993), Monger and Journeay (1994), and Mahoney et al. (1995).

Figure 3. Examples of basal till, Chehalis valley, southwestern British Columbia. a) Clast-rich till (unit 1) overlain by darker till with less abundant clasts (unit 2). Boxes indicate locations of Figures 3b and c. b) Close-up of unit 1 in Fig. 3a, showing weakly oxidized, dense till with silty sand matrix and about 35% clasts. c) Close-up of unit 2 in Fig. 3a, showing more oxidized, less dense till with sandy matrix and about 30% clasts. d) Close-up of till with sand- to granule-size oxidized sulphides, directly above the southeast wall of the Seneca pit.

GEOLOGY

Most of the Chehalis valley study area is underlain by intermediate and felsic volcanic-arc rocks of the Early to Middle Jurassic Harrison Lake Formation of the Harrison terrane in the Coast Belt of the southern Canadian Cordillera (Fig. 1; Monger, 1970; Arthur et al., 1993; Monger and Journeay, 1994; Mahoney et al., 1995). The volcanic rocks host several Kuroko-style massive sulphide occurrences, including the Seneca Zn-Cu-Pb deposit (McKinley et al., 1995). The Harrison terrane is intruded by Middle Jurassic porphyry stocks and plutons, made up of diorite, quartz diorite, granodiorite and tonalite, of the Coast Plutonic Complex to the west (Fig. 2).

METHODS

Three field duplicate pairs were randomly collected for till samples (2-3 kg; Fig. 3). Sample preparation was carried out and blind quality controls inserted at the British Columbia Geological Survey (BCGS). Till samples were dried in oven at 40°C and sieved to <0.063 mm fraction. Rock samples were jaw crushed and pulverized using a steel mill. All equipment was carefully washed between samples to avoid contamination. Elemental abundances were determined by portable X-ray fluorescence at BCGS; by aqua regia leaching- and lithium borate fusion-inductively coupled plasma mass spectrometry and emission spectrometry (ICP-MS/ES) at Acme Analytical Laboratories Ltd., Vancouver, B.C. (Acme); and by instrumental neutron activation analysis at Activation Laboratories Ltd., Ancaster, Ontario (Actlabs). Lead isotopic ratios for 2.5N HCl leachates (at room temperature for about 2 hours) from till and rock samples were measured after Pb purification by ion-exchange separation by MC-ICP-MS at the Pacific Centre for Isotopic and Geochemical Research (PCIGR), University of British Columbia; directly in bulk leachate solution with addition of dilute HNO_3 by HR-ICP-MS at Actlabs; and directly in bulk leachate solution by quadrupole ICP-MS (quad) at Acme. All Pb isotopic data were corrected for isobaric interference. The MC-ICP-MS results were corrected for mass fractionation and normalized to correct values for NIST NBS 981. The HR-ICP-MS results were also normalized to a Pb isotopic standard, whereas the quad data were not. Reproducibility and accuracy of the analyses were monitored by duplicate splits of <0.063 mm fraction of till samples (total 4 pairs) and international geological standards. Average relative difference from duplicates is 0.6% for $^{206}Pb/^{204}Pb$, $^{208}Pb/^{204}Pb$, and $^{207}Pb/^{206}Pb$, 1.2% for $^{207}Pb/^{204}Pb$, and 0.4% for $^{208}Pb/^{206}Pb$ for the HR-ICP-MS results; and 3.1% for $^{206}Pb/^{204}Pb$, 3.4% for $^{207}Pb/^{204}Pb$ and $^{208}Pb/^{206}Pb$, 1.8% for $^{208}Pb/^{204}Pb$, and 1.5% for $^{207}Pb/^{206}Pb$ for the quad results. Two times relative standard deviation uncertainties for the MC-ICP-MS results, based on 40 analyses of NIST NBS 981, are 0.010% for $^{206}Pb/^{204}Pb$ and $^{207}Pb/^{204}Pb$, 0.013% for $^{208}Pb/^{204}Pb$, 0.008% for $^{207}Pb/^{206}Pb$, and 0.011% for $^{208}Pb/^{206}Pb$. The Pb isotopic indicators of glacial dispersion are given as δ values calculated relative to the Seneca VMS values as follows:

$$\delta^{206}Pb/^{204}Pb = 1 - \frac{(^{206}Pb/^{204}Pb)_S - (^{206}Pb/^{204}Pb)_{VMS}}{(^{206}Pb/^{204}Pb)_{VMS}} \cdot 10^2 \qquad \delta^{208}Pb/^{204}Pb = 1 - \frac{(^{208}Pb/^{204}Pb)_S - (^{208}Pb/^{204}Pb)_{VMS}}{(^{208}Pb/^{204}Pb)_{VMS}} \cdot 10^2$$

$$\delta^{207}Pb/^{206}Pb = \frac{(^{207}Pb/^{206}Pb)_S - (^{207}Pb/^{206}Pb)_{VMS}}{(^{207}Pb/^{206}Pb)_{VMS}} \cdot 10^2 \qquad \delta^{208}Pb/^{206}Pb = \frac{(^{208}Pb/^{206}Pb)_S - (^{208}Pb/^{206}Pb)_{VMS}}{(^{208}Pb/^{206}Pb)_{VMS}} \cdot 10^2$$

where $(^{206}Pb/^{204}Pb)_s$, $(^{208}Pb/^{204}Pb)_s$, $(^{207}Pb/^{206}Pb)_s$, and $(^{208}Pb/^{206}Pb)_s$ are the isotopic ratios of till sample, $(^{206}Pb/^{204}Pb)_{VMS}$, $(^{208}Pb/^{204}Pb)_{VMS}$, $(^{207}Pb/^{206}Pb)_{VMS}$, and $(^{208}Pb/^{206}Pb)_{VMS}$ are the lowest $^{206}Pb/^{204}Pb$ and $^{208}Pb/^{204}Pb$, and the highest $^{207}Pb/^{206}Pb$ and $^{208}Pb/^{206}Pb$ ratios, respectively, of whole-rock analyses from the Seneca VMS deposit.

ELEMENTAL GEOCHEMISTRY

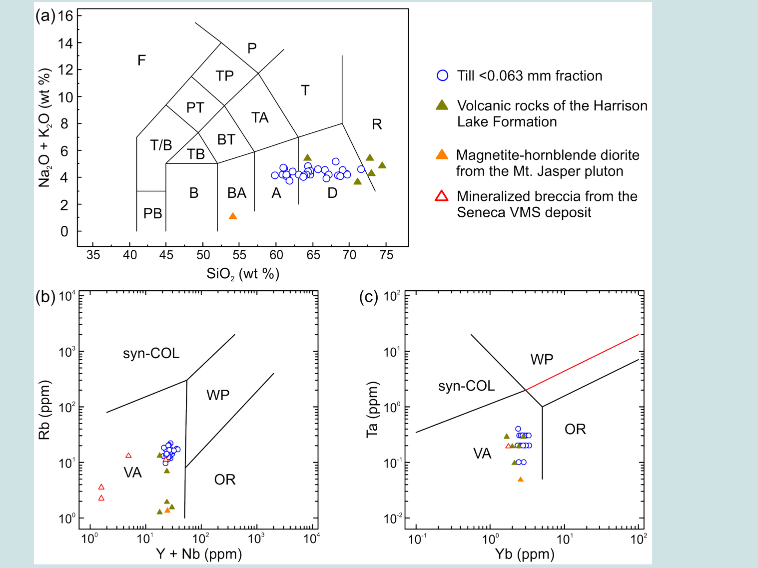

Figure 4. Geochemical discrimination diagrams for Chehalis valley rocks and tills, southwestern British Columbia. a) Total alkali ($Na_2O + K_2O$) vs. SiO_2 (anhydrous wt %) classification for volcanic rocks, showing the fields of andesite (A), basalt (B), basaltic andesite (BA), basaltic trachyandesite (BT), dacite (D), foidite (F), phonolite (P), picrobasalt (PB), phonotephrite (PT), rhyolite (R), trachyte and trachydacite (T), trachyandesite (TA), trachybasalt (TB), tephrite and basanite (T/B), and tephriphonolite (TP) after Le Bas et al. (1986). b) (Y + Nb) vs. Rb and c) Yb vs Ta felsic discrimination diagrams, showing the fields of volcanic arc (VA), syn-collisional (syn-COL), within plate (WP), and ocean ridge (OR) granites, and the boundary for OR granites from anomalous ridges (red line) after Pearce et al. (1984).

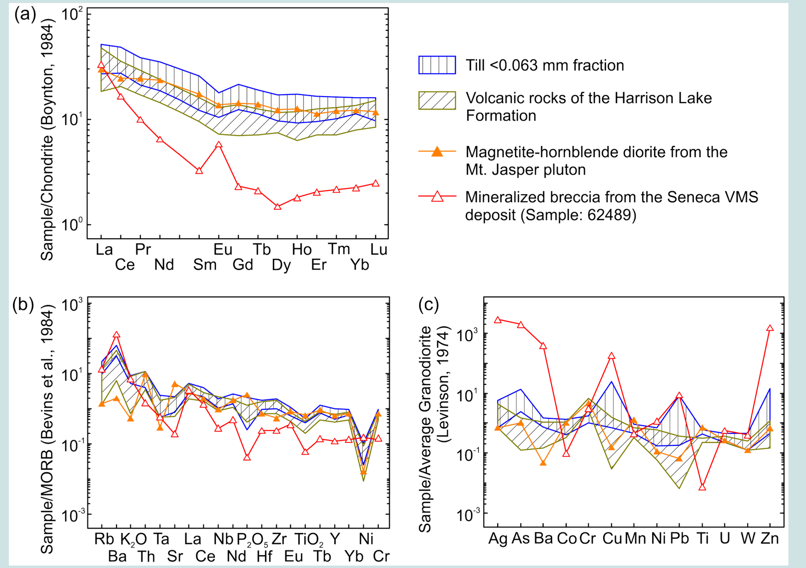

Figure 5. Spidergrams for Chehalis valley rocks and tills, southwestern British Columbia. a) Chondrite-normalized rare earth element plot, using normalization of Boynton (1984). b) Mid-ocean ridge basalt (MORB)-normalized spider plot, using normalization of Bevins et al. (1984). c) Average granodiorite-normalized spider plot, using normalization of Levinson (1974).

LEAD ISOTOPIC RESULTS

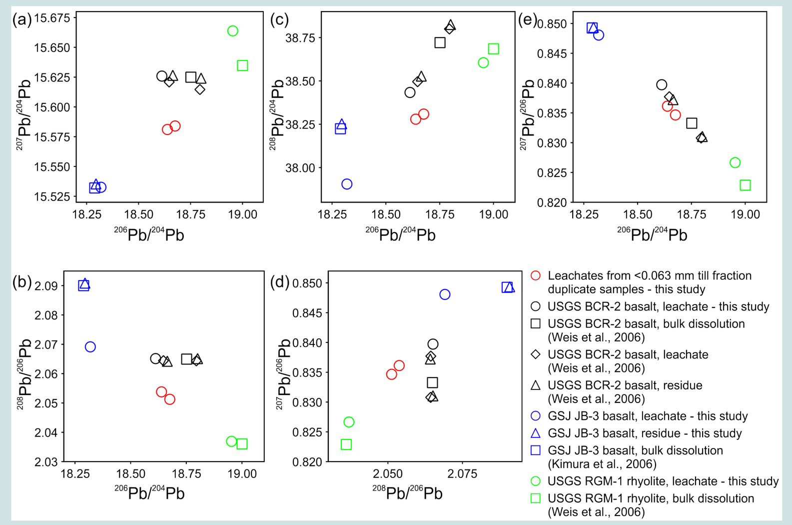

Figure 6. Pb-Pb isotopic plots showing multi-collector inductively-coupled plasma mass spectrometry results for leachates from Chehalis valley till <0.063 mm-fraction duplicate pair and for leachate-residue from international rock standards. Uncertainties are smaller than the size of the symbols. Literature leachate-residue and bulk-dissolution analyses for the standards are shown for comparison. a) $^{207}Pb/^{204}Pb$ vs. $^{206}Pb/^{204}Pb$; b) $^{208}Pb/^{206}Pb$ vs. $^{206}Pb/^{204}Pb$; c) $^{208}Pb/^{204}Pb$ vs. $^{206}Pb/^{204}Pb$; d) $^{207}Pb/^{206}Pb$ vs. $^{208}Pb/^{206}Pb$; e) $^{207}Pb/^{206}Pb$ vs. $^{206}Pb/^{204}Pb$.

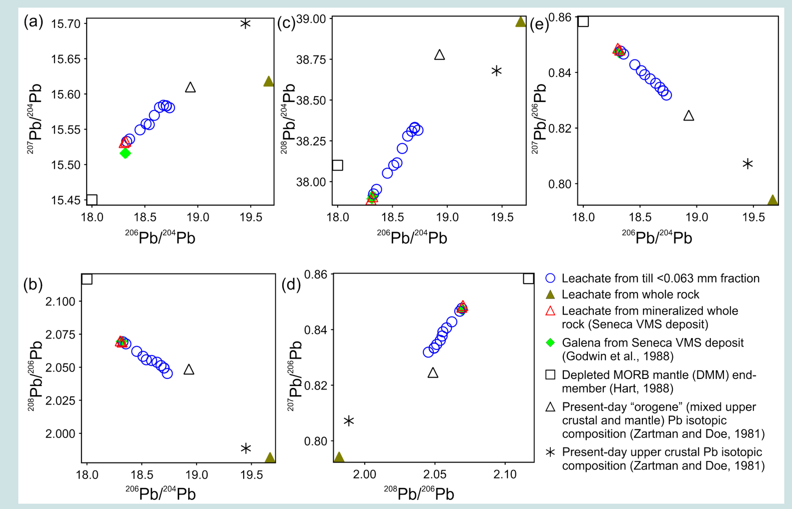

Figure 7. Pb-Pb isotopic plots showing multi-collector inductively-coupled plasma mass spectrometry results for leachates from Chehalis valley till <0.063 mm-fraction and whole-rock samples. Uncertainties are smaller than the size of the symbols. Literature galena analyses from the Seneca deposit and the present-day Pb isotopic compositions for depleted mid-ocean ridge basalt (MORB) mantle end-member, upper crustal, and "orogene" (mixed upper crust and mantle) reservoirs are shown for comparison. a) $^{207}Pb/^{204}Pb$ vs. $^{206}Pb/^{204}Pb$; b) $^{208}Pb/^{206}Pb$ vs. $^{206}Pb/^{204}Pb$; c) $^{208}Pb/^{204}Pb$ vs. $^{206}Pb/^{204}Pb$; d) $^{207}Pb/^{206}Pb$ vs. $^{208}Pb/^{206}Pb$; e) $^{207}Pb/^{206}Pb$ vs. $^{206}Pb/^{204}Pb$.

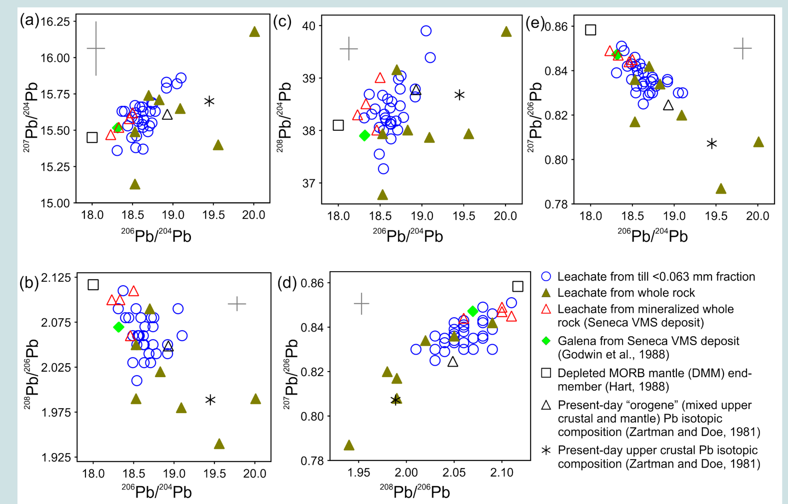
Figure 8. Pb-Pb isotopic plots showing high-resolution inductively-coupled plasma mass spectrometry results for leachates from Chehalis valley till <0.063 mm-fraction and whole-rock samples. Uncertainty bars show average relative difference from till <0.063 mm-fraction duplicates. Literature galena analyses from the Seneca deposit and the present-day Pb isotopic compositions for depleted mid-ocean ridge basalt (MORB) mantle end-member, upper crustal, and "orogene" (mixed upper crust and mantle) reservoirs are shown for comparison. a) $^{207}Pb/^{204}Pb$ vs. $^{206}Pb/^{204}Pb$; b) $^{208}Pb/^{206}Pb$ vs. $^{206}Pb/^{204}Pb$; c) $^{208}Pb/^{204}Pb$ vs. $^{206}Pb/^{204}Pb$; d) $^{207}Pb/^{206}Pb$ vs. $^{208}Pb/^{206}Pb$; e) $^{207}Pb/^{206}Pb$ vs. $^{206}Pb/^{204}Pb$.

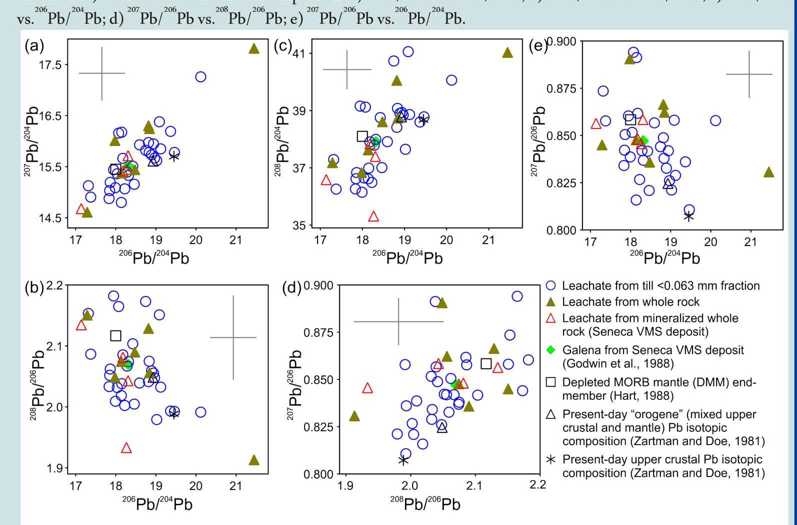
Figure 9. Pb-Pb isotopic plots showing quadrupole inductively-coupled plasma mass spectrometry results for leachates from Chehalis valley till <0.063 mm-fraction and whole-rock samples. Uncertainty bars show average relative difference from till <0.063 mm-fraction duplicates. Literature galena analyses from the Seneca deposit and the present-day Pb isotopic compositions for depleted mid-ocean ridge basalt (MORB) mantle end-member, upper crustal, and "orogene" (mixed upper crust and mantle) reservoirs are shown for comparison. a) $^{207}Pb/^{204}Pb$ vs. $^{206}Pb/^{204}Pb$; b) $^{208}Pb/^{206}Pb$ vs. $^{206}Pb/^{204}Pb$; c) $^{208}Pb/^{204}Pb$ vs. $^{206}Pb/^{204}Pb$; d) $^{207}Pb/^{206}Pb$ vs. $^{208}Pb/^{206}Pb$; e) $^{207}Pb/^{206}Pb$ vs. $^{206}Pb/^{204}Pb$.

BINARY MIXING MODELS

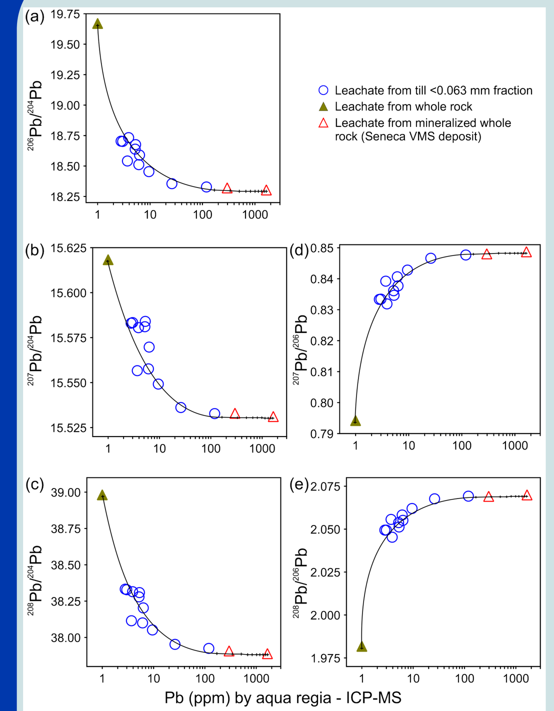

Figure 10. Plots of Pb isotopic ratios by multi-collector inductively coupled plasma mass spectrometry vs. Pb concentrations for leachates from Chehalis valley till <0.063 mm-fraction and whole-rock samples showing binary mixing models (after Langmuir et al., 1978). Ticks on the model curves mark 10% increments. Pb concentrations are by aqua regia-inductively coupled plasma mass spectrometry. Uncertainties are smaller than the size of the symbols. a) Pb (ppm) vs. $^{206}Pb/^{204}Pb$; b) Pb (ppm) vs. $^{207}Pb/^{204}Pb$; c) Pb (ppm) vs. $^{208}Pb/^{204}Pb$; d) Pb (ppm) vs. $^{207}Pb/^{206}Pb$; e) Pb (ppm) vs. $^{208}Pb/^{206}Pb$.

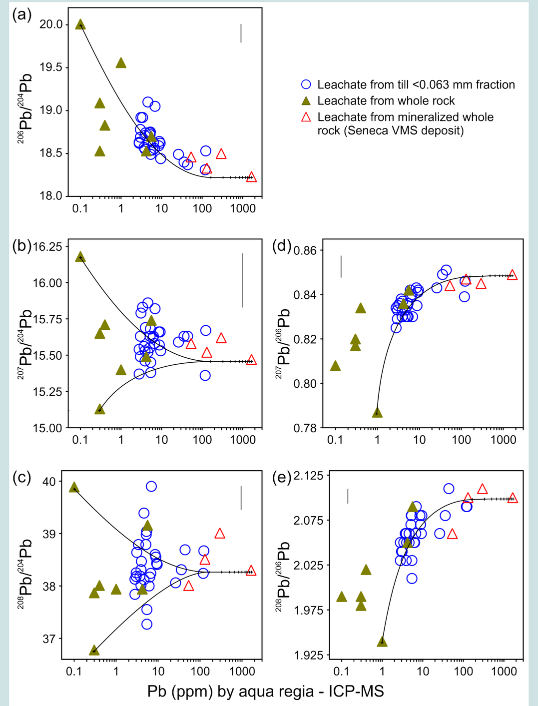

Figure 11. Plots of Pb isotopic ratios by high-resolution inductively-coupled plasma mass spectrometry vs. Pb concentrations for leachates from Chehalis valley till <0.063 mm-fraction and whole-rock samples showing binary mixing models (after Langmuir et al., 1978). Ticks on the model curves mark 10% increments. Pb concentrations are by aqua regia-inductively coupled plasma mass spectrometry. Uncertainty bars for isotopic ratios show average relative difference from till <0.063 mm-fraction duplicates. Average relative difference for Pb concentrations in the duplicates is smaller than the size of the symbols. a) Pb (ppm) vs. $^{206}Pb/^{204}Pb$; b) Pb (ppm) vs. $^{207}Pb/^{204}Pb$; c) Pb (ppm) vs. $^{208}Pb/^{204}Pb$; d) Pb (ppm) vs. $^{207}Pb/^{206}Pb$; e) Pb (ppm) vs. $^{208}Pb/^{206}Pb$.

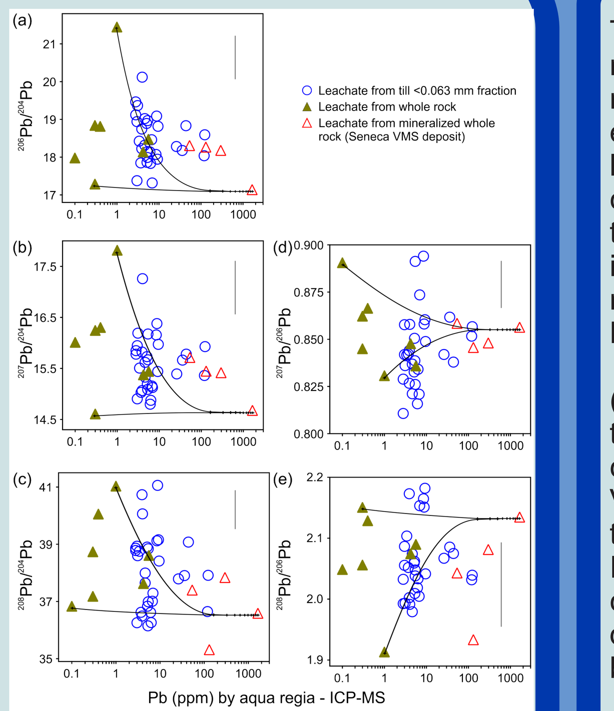

Figure 12. Plots of Pb isotopic ratios by quadrupole inductively-coupled plasma mass spectrometry vs. Pb concentrations for leachates from Chehalis valley till <0.063 mm-fraction and whole-rock samples showing binary mixing models (after Langmuir et al., 1978). Ticks on the model curves mark 10% increments. Pb concentrations are by aqua regia-inductively coupled plasma mass spectrometry. Uncertainty bars for isotopic ratios show average relative difference from till <0.063 mm-fraction duplicates. Average relative difference for Pb concentrations in the duplicates is smaller than the size of the symbols. a) Pb (ppm) vs. $^{206}Pb/^{204}Pb$; b) Pb (ppm) vs. $^{207}Pb/^{204}Pb$; c) Pb (ppm) vs. $^{208}Pb/^{204}Pb$; d) Pb (ppm) vs. $^{207}Pb/^{206}Pb$; e) Pb (ppm) vs. $^{208}Pb/^{206}Pb$.

INDICATORS OF GLACIAL DISPERSAL

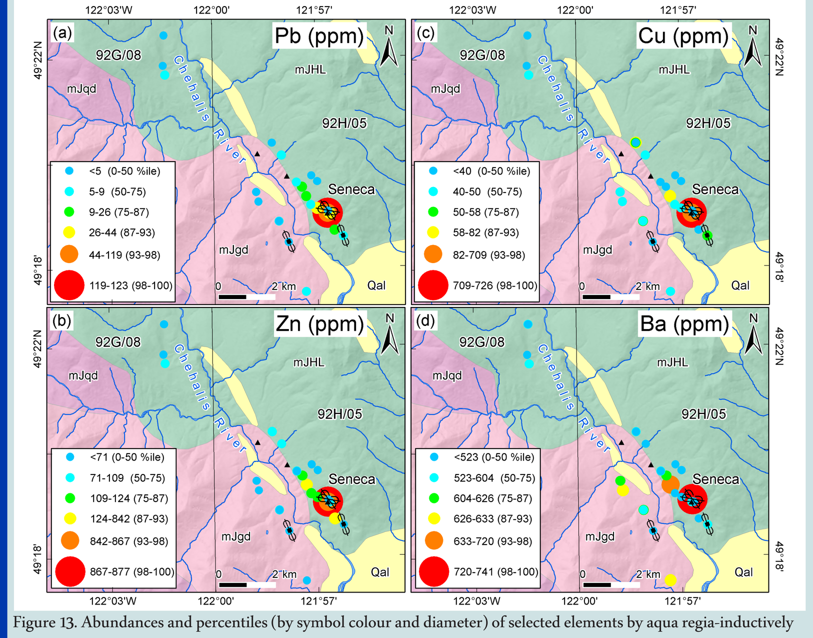

Figure 13. Abundances and percentiles (by symbol colour and diameter) of selected elements by aqua regia-inductively coupled plasma mass spectrometry from <0.063 mm fraction of till samples, Chehalis valley. Rock legend and other symbols as in Figure 2. a) Pb (ppm); b) Zn (ppm); c) Cu (ppm); d) Ba (ppm).

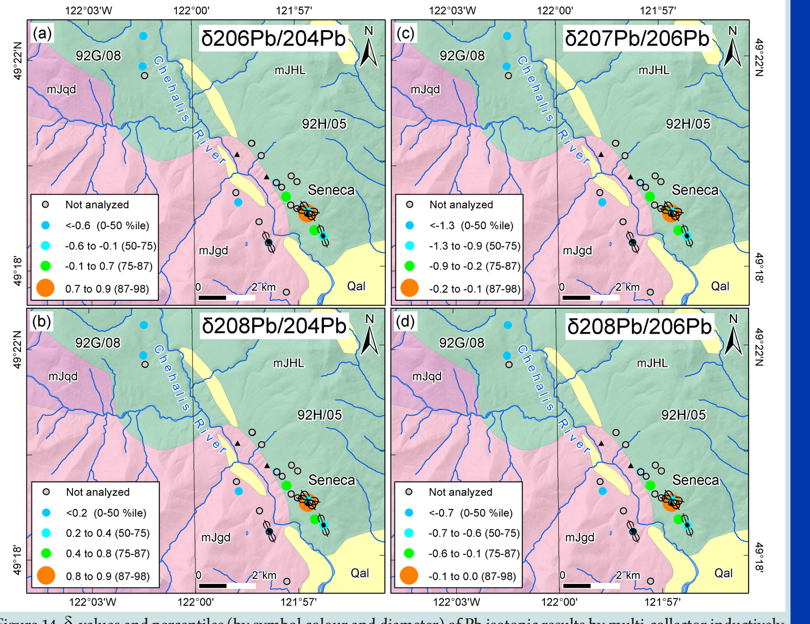

Figure 14. δ values and percentiles (by symbol colour and diameter) of Pb isotopic results by multi-collector inductively coupled plasma mass spectrometry for leachates from <0.063 mm fraction of till samples, Chehalis valley. The δ values are obtained by normalizing the isotopic ratios of sample to the least radiogenic ratio of whole-rock analyses from the Seneca VMS deposit (see text for detail). Rock legend and other symbols as in Figure 2. a) $\delta^{206}Pb/^{204}Pb$; b) $\delta^{208}Pb/^{204}Pb$; c) $\delta^{207}Pb/^{206}Pb$; d) $\delta^{208}Pb/^{206}Pb$.

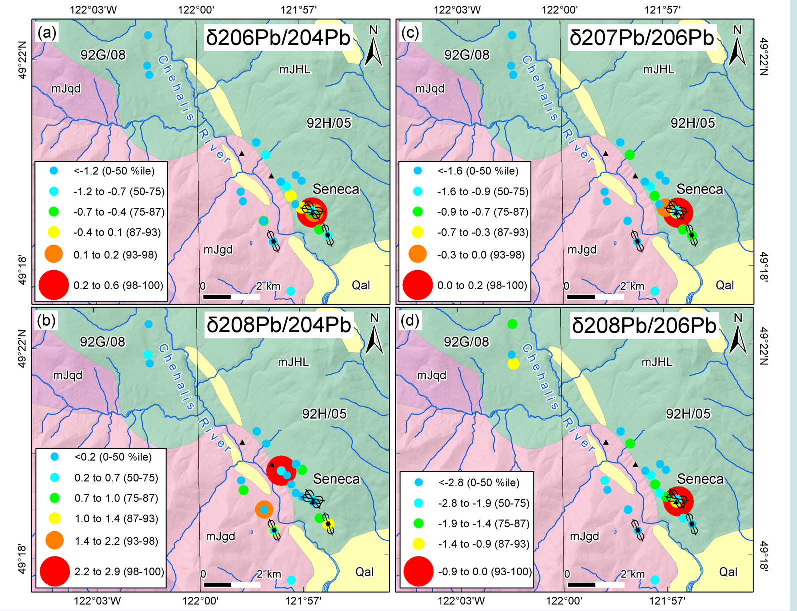

Figure 15. δ values and percentiles (by symbol colour and diameter) of Pb isotopic results by high-resolution inductively coupled plasma mass spectrometry for leachates from <0.063 mm fraction of till samples, Chehalis valley. The δ values are obtained by normalizing the isotopic ratios of sample to the least radiogenic ratio of whole-rock analyses from the Seneca VMS deposit (see text for detail). Rock legend and other symbols as in Figure 2. a) $\delta^{206}Pb/^{204}Pb$; b) $\delta^{208}Pb/^{204}Pb$; c) $\delta^{207}Pb/^{206}Pb$; d) $\delta^{208}Pb/^{206}Pb$.

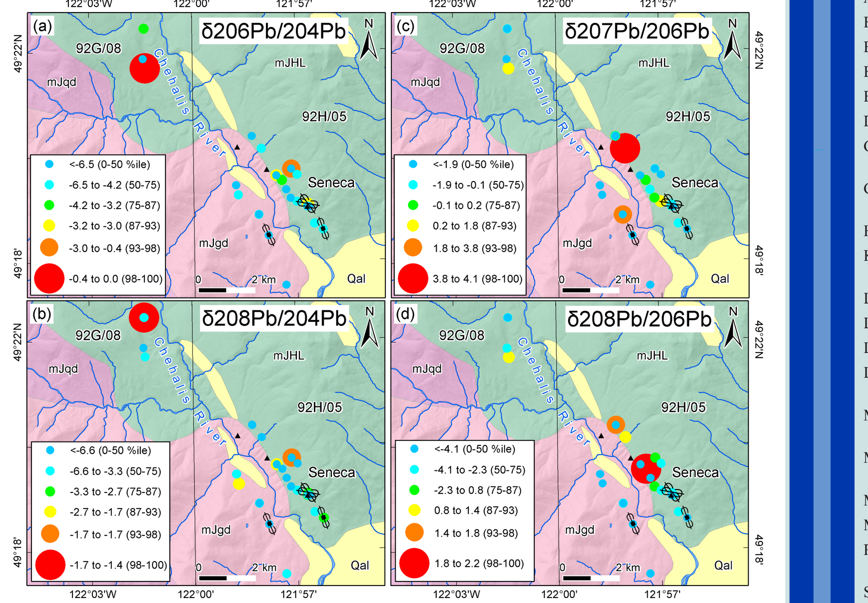

Figure 16. δ values and percentiles (by symbol colour and diameter) of Pb isotopic results by quadrupole inductively coupled plasma mass spectrometry for leachates from <0.063 mm fraction of till samples, Chehalis valley. The δ values are obtained by normalizing the isotopic ratios of sample to the least radiogenic ratio of whole-rock analyses from the Seneca VMS deposit (see text for detail). Rock legend and other symbols as in Figure 2. a) $\delta^{206}Pb/^{204}Pb$; b) $\delta^{208}Pb/^{204}Pb$; c) $\delta^{207}Pb/^{206}Pb$; d) $\delta^{208}Pb/^{206}Pb$.

SUMMARY AND CONCLUSIONS

The Pb isotopic results for 2.5N HCl leachates from Chehalis valley tills (<0.063 mm fraction), and VMS mineralization and the surrounding volcanic-arc rocks (Figs. 4 and 5) show 3-9% difference. This is 2-3 orders of magnitude above the uncertainties of the state-of-the-art MC-ICP-MS analyses on leachate Pb purified by ion-exchange separation (Figs. 6 and 7), and 8-20 times the uncertainties of the HR-ICP-MS analyses directly on bulk leachate (Fig. 8). The large Pb isotopic contrast between Chehalis valley VMS mineralization and the background crust, well above the uncertainties of the Pb isotopic results, makes Pb isotopes from till leachates suitable for tracing of down-ice glacial dispersal for as young as the Mesozoic deposits in Cordillera. For the direct-leachate Pb isotopic results using more widely available quad instrumentation, the analytical uncertainties of the raw Pb isotopic ratios, uncorrected for mass bias, are 2-9 times those of the HR-ICP-MS and 140-340 times those of the MC-ICP-MS (Fig. 9)

Data arrays shown in the Pb abundance vs. Pb isotopic ratio diagrams by MC-ICP-MS are consistent with mixing (after Langmuir et al., 1978) of two distinct end-member compositions (Fig. 10). One of the end members, having the lowest $^{206}Pb/^{204}Pb$, $^{207}Pb/^{204}Pb$, and $^{208}Pb/^{204}Pb$ ratios, and the highest $^{207}Pb/^{206}Pb$ and $^{208}Pb/^{206}Pb$ ratios, and Pb content, is similar to the isotopic composition of galena from the Seneca deposit (Godwin, 1988) and represents the VMS mineralization. The second end member, having the highest $^{206}Pb/^{204}Pb$, $^{207}Pb/^{204}Pb$, and $^{208}Pb/^{204}Pb$ ratios, and the lowest $^{207}Pb/^{206}Pb$ and $^{208}Pb/^{206}Pb$ ratios, and Pb content, is the background crust. The Pb isotopic results by HR-ICP-MS and quadrupole ICP-MS show more scattered isotopic ratios from tills and rocks with decreasing Pb concentration, indicating isotopically heterogeneous background crustal materials (Figs. 11 and 12). The larger datasets by these methods are consistent with the model that Chehalis valley tills are derived from the local bedrock sources and have variable proportions of Pb derived from the isotopically distinct VMS mineralization.

Near-linear arrays of till and rock analyses by MC-ICP-MS shown in the Pb-Pb isotopic ratio diagrams (Fig. 7) are consistent with binary mixing of isotopically heterogeneous materials. If interpreted as a secondary isochron, the slope of the linear array (n = 13; excluding diorite analysis from Mt. Jasper pluton) shown in the $^{207}Pb/^{204}Pb$ vs. $^{206}Pb/^{204}Pb$ diagram (Fig. 7a) corresponds to an age of 2131±180 Ma (95% confidence), with the lower intercept of the Stacey and Kramers (1975) growth curve at 2271 Ma. The mean square of the weighted deviates (MSWD) of 28 indicates that not all of the data points fit a straight line within the estimated uncertainties. This age is much older than the age of the Seneca VMS deposit and the surrounding volcanic-arc rocks (middle Jurassic) but falls within the range of the Paleoproterozoic ages of the major crust-forming events worldwide. If the linear array had a geochronological significance, it would imply that both the Seneca VMS deposit and the background volcanic-arc rocks shared the same, closed-system Paleoproterozoic source, such as a sub-continental lithosphere. However, the Pb-Pb isotopic results by HR-ICP-MS from more till and rock samples are more scattered, suggesting a mixture of leads in the tills derived from the VMS mineralization and isotopically heterogeneous crustal sources (Fig. 8).

Elemental abundances for 2.5N HCl leachates from Chehalis valley <0.063 mm fraction of basal till highlight down-ice glacial dispersal from the known VMS occurrences. Although Pb, Zn, Cu, and Ba abundances are enriched in the Seneca VMS deposit 10-1000 times typical crustal values (Fig. 5b and c), they show inconsistent till anomalies (Fig. 13). In contrast, Pb isotopic ratios appear to be effective indicators of the glacial dispersal for the VMS deposits (Fig. 14). For the direct analyses of bulk leachates by HR-ICP-MS, the $^{206}Pb/^{204}Pb$ and $^{207}Pb/^{206}Pb$ ratios are consistent with the state-of-the-art MC-ICP-MS results and can be used as glacial dispersal indicators for the VMS deposits (Fig. 15). In the case of the quad direct-leachate Pb isotopic results, the analytical uncertainties may be too large for tracing <10% isotopic contrast (Fig. 16).

ACKNOWLEDGEMENTS

We thank Tyler Ruks (former University of British Columbia) and Brent Ward (Simon Fraser University) for insightful discussions of VMS occurrences in southwestern British Columbia and Quaternary geology of the Chehalis valley, and Dominique Weis (University of British Columbia), Bruno Kieffer (University of British Columbia), Liyan Xing (University of British Columbia), John Gravel (Acme Analytical Laboratories Ltd.), Bill MacFarlane (Acme Analytical Laboratories Ltd.), Eric Hoffman (Activation Laboratories Ltd.), and Yakov Kapusta (Activation Laboratories Ltd.) for help with the analytical work.

REFERENCES

Arthur, A.J., Smith, P.L., Monger, J.W.H., Tipper, H.W., 1993. Mesozoic stratigraphy and Jurassic paleontology west of Harrison Lake, southwestern British Columbia. Geological Survey of Canada, Bulletin 441, 67 p.

Bell, K., Franklin, J.M., 1993. Application of lead isotopes to mineral exploration in glaciated terrains. Geology 21, 1143–1146.

Bell, K., Murton, J.B., 1995. A new indicator of glacial dispersal: lead isotopes. Quaternary Science Reviews 14, 275–287.

Bevins, R.E., Kokelaar, B.P., Dunkley, P.N., 1984. Petrology and geochemistry for lower to middle Ordovician igneous rocks in Wales: A volcanic arc to marginal basin transition. Proceedings of the Geologists Association 95, 337–347.

Boynton, W.V., 1984. Geochemistry of the rare earth elements: Meteorite studies. In: Rare Earth Element Geochemistry, P. Henderson (ed.), Elsevier, New York, pp. 63–114.

DiLabio, R.N.W., 1990. Glacial dispersal trains. In: Glacial Indicator Tracing, R. Kujansuu and M., Saamisto (eds.), A.A. Balkema, Rotterdam, p. 109–122.

Gabrielse, H., Monger, J.W.H., Wheeler, J.O., Yorath, C.J., 1991. Part A – Morphogeological belts , tectonic assemblages and terranes, Chapter 2. In: Geology of the Cordilleran Orogen in Canada, H. Gabrielse and C.J. Yorath (eds.), Geological Society of America, The Geology of North America G-2, Geological Survey of Canada, Geology of Canada 4, pp. 15–28.

Godwin, C.I., Gabites, J.E., Andrew, A., 1988. Leadtable: a galena lead isotope database for the Canadian Cordillera, with a guide to its use by explorationists. British Columbia Ministry of Energy, Mines and Petroleum Resources, British Columbia Geological Survey Paper 1988-4, 187 p.

Hart, S.R., 1988. Heterogeneous mantle domains: signatures, genesis and mixing chronologies. Earth and Planetary Science Letters 90 (3), 273–296.

Kimura, J.-I., Sisson, T.W., Nakano, N., Coombs, M.L., Lipman, P.W., 2006. Isotope geochemistry of early Kilauea magmas from the submarine Hilina bench: The nature of the Hilina mantle component. Journal of Volcanology and Geothermal Research 151, 51–72.

Langmuir, C.H., Vocke, R.D., Jr., Gilbert, N.H., Stanley, R.H., 1978. A general mixing equation with applications to Icelandic basalts. Earth and Planetary Science Letters 37, 380–392.

Le Bas, M.J., Le Maitre, R.W., Streckeisen, A., Zanettin, B., 1986. A chemical classification of volcanic rocks based on the total alkali-silica diagram. Journal of Petrology 27, 745–750.

Levinson, A.A., 1974. Introduction to Exploration Geochemistry. Applied Publ. Ltd., Calgary, 612 p.

Levson, V.M., 2001. Regional till geochemical surveys in the Canadian Cordillera: sample media, methods, and anomaly evaluation. In: Drift Exploration in Glaciated Terrain, M.B. McClenaghan, P.T. Bobrowsky, G.E.M. Hall and S.J. Cook (eds.), The Geological Society of London, Special Publication 185, pp. 45–68.

Mahoney, J.B., Friedman, R.M., McKinley, S.D., 1995. Evolution of a Middle Jurassic volcanic arc: stratigraphic, isotopic, and geochemical characteristics of the Harrison Lake Formation, southwestern British Columbia. Canadian Journal of Earth Sciences 32, 1759–1776.

McKinley, S., Thompson, J.F.H., Barrett, T.J., 1995. Volcanic stratigraphy and lithogeochemistry of the Seneca Prospect, southwestern British Columbia (92H/5W). In: Geological Fieldwork 1994, British Columbia Ministry of Energy, Mines and Petroleum Resources, British Columbia Geological Survey Paper 1995-1, pp. 503–512.

Monger, J.W.H., 1970. Hope map area, west half (92H W1/2), British Columbia. Geological Survey of Canada, Paper 69-47, 75 p.

Monger, J.W.H., Journeay, J.M., 1994. Guide to the geology and tectonic evolution of the southern Coast Mountains. Geological Survey of Canada, Open File 2490, 81 p.

Pearce, J.A., Harris, N.B.W., Tindle, A.G., 1984. Trace element discrimination diagrams for the tectonic interpretation of granitic rocks. Journal of Petrology 25, 956–983.all and S.J. Cook (eds.), The Geological Society of London, Special Publication 185, pp. 45–68.

Shilts, W.W., 1976. Glacial till and mineral exploration. In: Glacial Till, R.F. Legett (ed.), Royal Society of Canada, Special Publication 12, pp. 205–233.

Simonetti, A., Bell, K., Hall, G.E.M., 1996. Pb isotopic ratios and elemental abundances for selective leachates from near-surface till: implications for mineral exploration, Applied Geochemistry 11, 721–734.

Stacey, J.S., Kramers, J.D., 1975. Approximation of terrestrial lead isotope evolution by a two-stage model. Earth and Planetary Science Letters 26 (2), 207–221.

Weis, D., Kieffer, B., Maerschalk, C., Barling, J., De Jong, J., Williams, G., Hanano, D., Pretorius, W., Mattielli, N., Scoates, J.S., Goolaerts, A., Friedman, R., Mahoney, J.B., 2006. High-precision isotopic characterization of USGS reference materials by TIMS and MC-ICP-MS. Geochemistry, Geophysics, Geosystems 7 (8), Q08006, doi:10.1029/2006GC001283.

Zartman, R.E., Doe, B.R., 1981. Plumbotectonics – the model. Tectonophysics 75, 135–162.